Chapter 3

Monitoring of the 2008 Chaitén Eruption Cloud Using MODIS Data and its Impacts

Yuanzhi Zhang, Jin Yeu Tsou, Zhaojun Huang,
Jinrong Hu and Wyss W.-S. Yim

Additional information is available at the end of the chapter

http://dx.doi.org/10.5772/00000

Abstract

This chapter presents the monitoring of the 2008 Chaitén eruption cloud using Moderate Resolution Imaging Spectroradiometer (MODIS) data and its impacts. The 8-day MODIS data from 3 to 10 May 2008 were used to track the movement and dispersion of the eruption cloud of the Chaitén volcano in Chile following the eruption on 2 May 2008. For detecting volcanic particulates, the procedure is adopted based on the brightness temperature difference (BTD) algorithm, by which the thermal infrared channels were centered on 11–12 μm of multispectral satellite sensors. The BTD is generally negative for volcanic ash but positive for ice and water vapor. The eruption cloud was found to drift northeastward, eastward, and southeastward crossing the central and northern part of Argentina and over the Atlantic Ocean. The timing of heavy rainfall in South Africa during May–June, in central Australia during June 2008 and in Hong Kong during June (the wettest since record began in 1884), was considered to have been connected to the dispersion of the particulates from this Chaitén eruption to further impact downstream.

Keywords: volcanic cloud dispersion, MODIS data, Chaitén eruption, heavy rainfall

1. Introduction

Volcanic eruption clouds are potentially hazardous to aircrafts in the air. The ash clouds may persist for many hours or perhaps days and have been known to produce en route flight diversions in regions thousands of kilometers from their source in [1]. As volcanic eruptions are variable in intensity and composition, the tracking of the eruption cloud is particularly relevant to aviation safety. Additionally, the spread of eruption clouds may have possible climatic effects including precipitation changes. Due to the isolated locations of many volcanoes, remote sensing plays an important role in tracking ash clouds as they drift away from an erupting volcano. In this paper, Moderate Resolution Imaging Spectroradiometer (MODIS) data were downloaded from 3 to 10 May to monitor and retrieve the volcanic ash cloud from the 2 May eruption of Chaitén volcano in Chile and to analyze its impacts on rainfall.

Figure 1. Map of southern South America showing the location of the Chaitén Volcano.

The Chaitén volcano, a southern Andean arc volcano in Chile located at latitude 42.833°S and longitude 72.646°W (**Figure 1**), began erupting explosively in the early morning around 08:00 coordinated universal time (UT) on 2 May 2008 in [2], without warning in [3]. Ash columns abruptly jetted from the volcano into the stratosphere reaching an altitude of more than 21 km followed by lava dome effusion and continuous low-altitude close space ash plumes in [4]. This eruption was the largest eruption in Chile since Cerro Hudson in 1991 in [5] and the largest explosive rhyolitic eruption since Novarupta, Alaska in 1912. Prior to this, the volcano comprised a rhyolitic lava dome within a 2.5 km diameter caldera was last thought to have erupted at 9370 ^{14}C years B.P. in [6]. The eruption had immediate and serious social and economic consequences across southern Chile and Argentina. Floods and lahars inundated the town of Chaitén and its 4625 residents were evacuated. Widespread ashfall and drifting ash clouds closed regional airports and led to the cancellation of numerous domestic and international flights in Argentina and Chile in [7]. Furthermore, the aquaculture industry in the nearby Gulf of Corcovado was badly affected, while ecotourism was curtailed and the regional nature reserves were forced to close.

2. Data and methodology

2.1. Data

In this study, the 8-day data of (from 3 to 10 May 2008) NASA-MODIS Level-1B Calibrated Geolocation Data Set (MOD02) in [8] with 1 km resolution were applied to track the movement and dispersion of the eruption cloud of the Chaitén volcano in Chile following the eruption on 2 May 2008. About 30-year average rainfall distribution image and June 2008 rainfall image were used to compare with the drought information, which was downloaded from the website of Australian Bureau of Meteorology. And the rainfall images for South Africa and annual rainfall data for Hong Kong were downloaded from the websites of South Africa Weather Service and Hong Kong Observatory, respectively.

2.2. Methods

2.2.1. Methodology for volcanic ash tracking

The most widely used approach to detect volcanic ash is based on the brightness temperature difference (BTD) procedure applied to the channels centered at around 11 and 12 μm in [9]. The BTD technique has been applied either to polar satellite instruments such as the Advanced Very High Resolution Radiometer (AVHRR) [10–11], the Moderate Resolution Imaging Spectroradiometer (MODIS) [12–17], rather than to geostationary satellite instruments as the Geostationary Operational Environmental Satellite (GOES) in [18], and the Spin Enhanced Visible and Infrared Imager (SEVIRI) measurements in [19]. In this study, the volcanic ash detection procedure adopted is based on the BTD algorithm using the thermal infrared channels centered on 11 μm and 12 μm of a multispectral satellite sensor. This is because volcanic ash contains large amounts of silicates that scatter and absorb infrared radiation in a different way than meteorological water and ice clouds in [20]. A BTD of 11–12 μm is generally negative for volcanic ash and dust and positive for ice and water clouds [11, 20, 21]. Bands 31

(11 μm) and 32 (12 μm) of MODIS data were used for volcanic ash monitoring in this study. Before BTD calculation, there are two steps. Firstly, Digital Number (DN) values need to be transferred into radiant intensity to calculate the brightness temperature since MODIS images are expressed with DN values. Secondly, brightness temperature was calculated using the Planck function.

The formulae used for Radiant Intensity calculation of bands 31 and 32 of MODIS data were used as in [22]:

$$\mathrm{Rad}\,31 = \mathrm{scale}\,31(\mathrm{band}\,31 - \mathrm{offset}\,31) \quad (1)$$

$$\mathrm{Rad}\,32 = \mathrm{scale}\,32(\mathrm{band}\,32 - \mathrm{offset}\,32) \quad (2)$$

(where rad 31 and rad 32 are the Heat Radiant Intensity ($Wm^{-2}.sr^{-1}(m^{-1})$) of bands 31 and 32 of MODIS data, respectively; while band 31 and band 32 are the DN values of band 31 and 32 of MODIS data, respectively; scale 31 and offset 31 are the radiometric calibration constant of band 31 of MODIS data, and, scale 32 and offset 32 are the radiometric calibration constant of band 32 of MODIS data).

After determination of the Heat Radiant Intensity, the brightness temperature can be calculated based on Plank function. The formulae used were used as in [22]:

$$T\,31 = K\,31,2 / \ln(1 + K\,31,1 / \mathrm{rad}\,31) \quad (3)$$

$$T\,32 = K\,32,2 / \ln(1 + K\,32,1 / \mathrm{rad}\,32) \quad (4)$$

(where K 31,1 = 729.541636 $W.m^{-2}.sr^{-1}.\mu m^{-1}$; K 31,2 = 1304.413871K; K 32, 1 = 474.684780 $W.m^{-2}.sr^{-1}.\ \mu m^{-1}$, and, K 32, 2 = 1196.978785K).

2.2.2. Methodology for rainfall study

In this study, Australian, South Africa, and Hong Kong history observation rainfall data were downloaded to study the impacts of Chaitén volcano eruption cloud on rainfall. For Australia, the average rainfall in June from 1961 to 1990 and rainfall in June 2008 were obtained as shown in **Figure 2** and **Figure 3**. For South Africa, the rainfall data of May and June were downloaded to compare the rainfall change caused by Chaitén volcanic ash migration as shown in **Figure 4** and **Figure 5**. For Hong Kong, the historical rainfall data used in this study is the annual rainfall data between 1947 and 2009 obtained from Hong Kong Observatory as shown in **Figure 6**. The figure also listed out the significant annual rainfall change of Hong Kong caused by volcanic eruptions or nuclear tests.

http://dx.doi.org/10.5772/00000

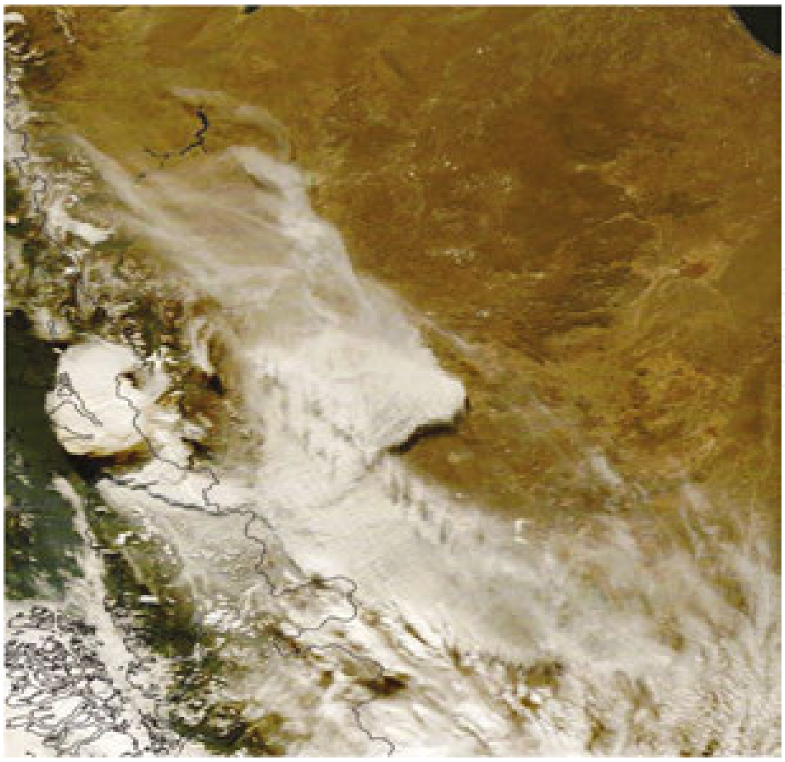

Figure 2. Average rainfall in June over the Australian continent from 1961 to 1990 (Courtesy of Australian Bureau of Meteorology).

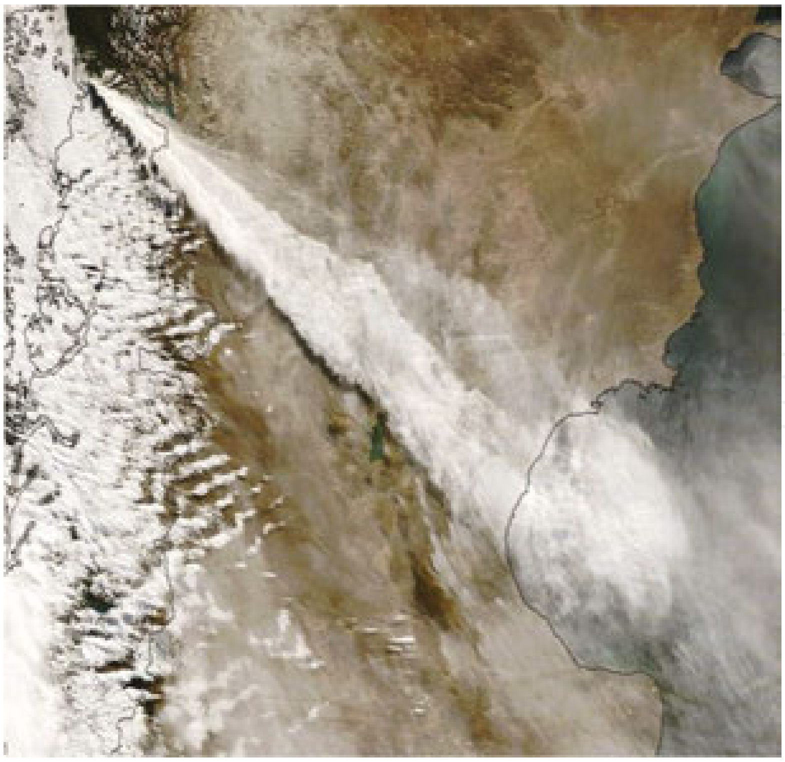

Figure 3. Heavy rainfall in June 2008 in Australia (Courtesy of Australian Bureau Meteorology).

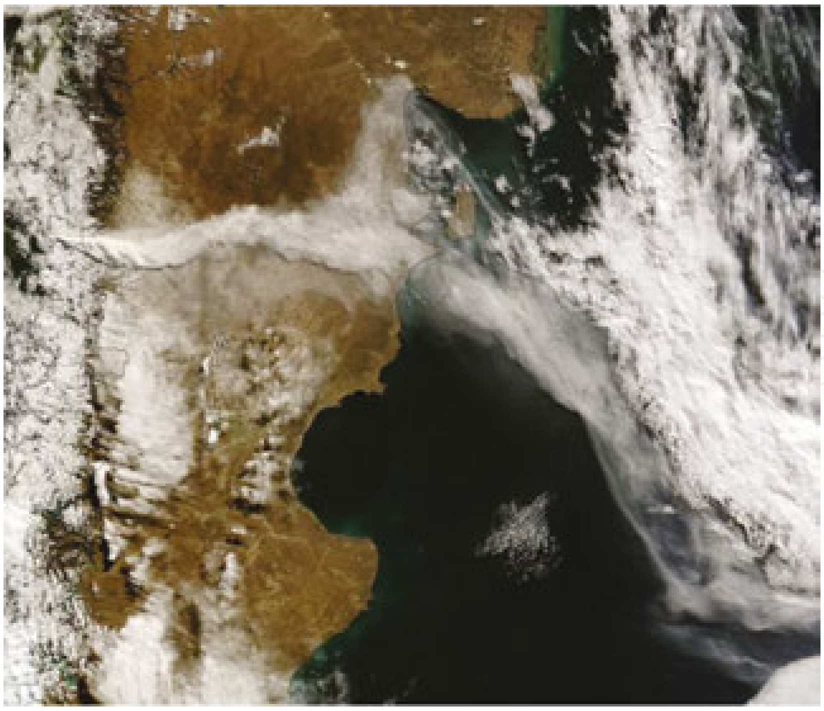

Figure 4. Rainfall May 2008 in South Africa, but a significant increasing rainfall during 21–31 May was attributed to the migration of the eruption cloud from the Chaitén volcano in Chile following the eruption on 2 May 2008 (Courtesy of South Africa Weather Service).

Figure 5. Rainfall in June 2008 in South Africa, but a heavy rainfall was attributed to the migration of the eruption cloud from the Chaitén volcano in Chile following the eruption on 2 May 2008 (Courtesy of South Africa Weather Service).

http://dx.doi.org/10.5772/00000

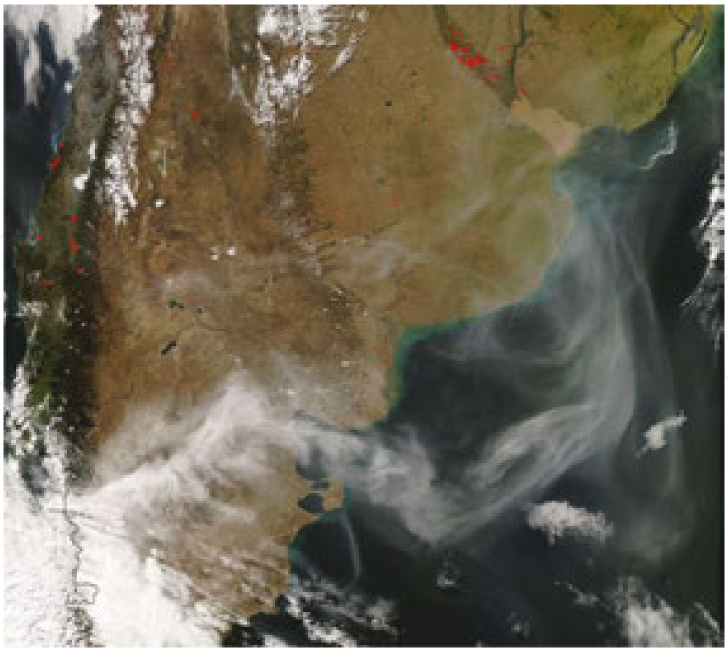

Figure 6. The annual rainfall of Hong Kong from 1947 to 2009 (Courtesy of the Hong Kong Observatory).

3. Satellite tracking of eruption cloud

Images of the eruption cloud recorded by NASA-MODIS using the Terra and Aqua MODIS sensors are shown as examples as in **Figures 7–12**.

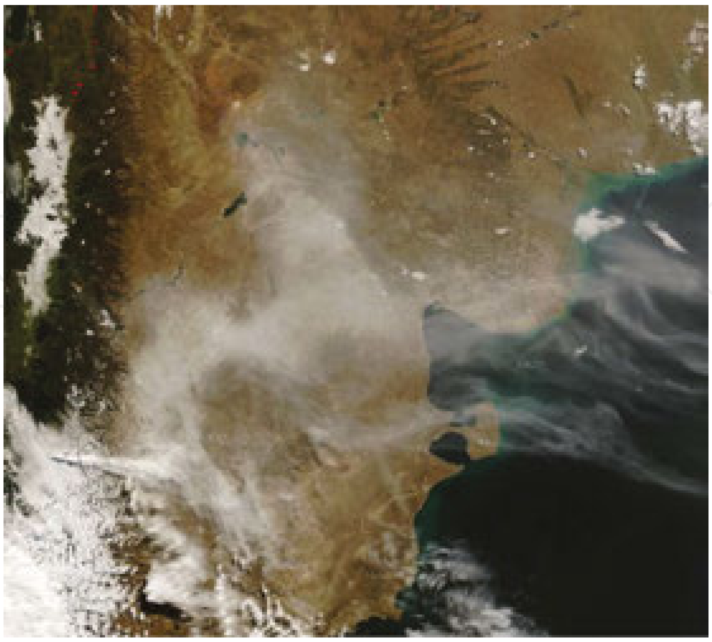

Figure 7. May 2, 13:50 UT: Chile (MODIS).

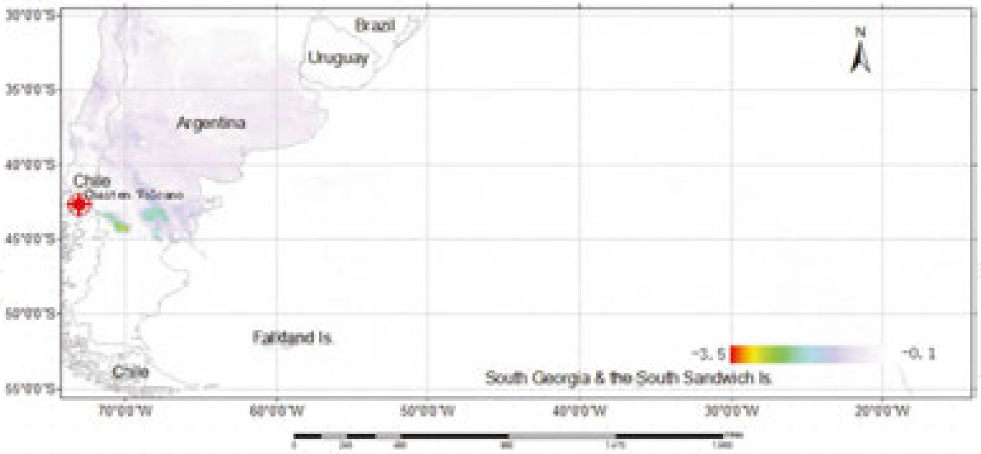

Figure 8. May 3, 14:35 UT: Chile (MODIS).

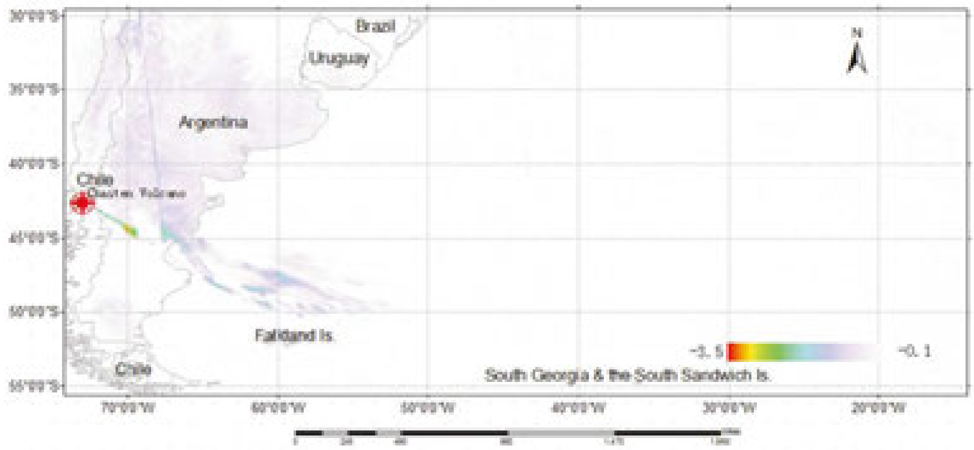

Figure 9. May 5, 14:25 UT: Chile (MODIS).

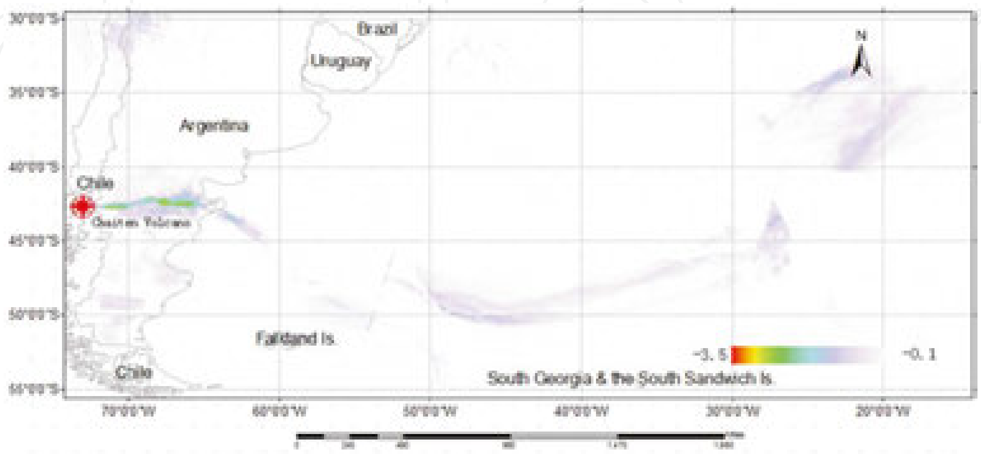

Figure 10. May 6, 15:05 UT: Chile (MODIS).

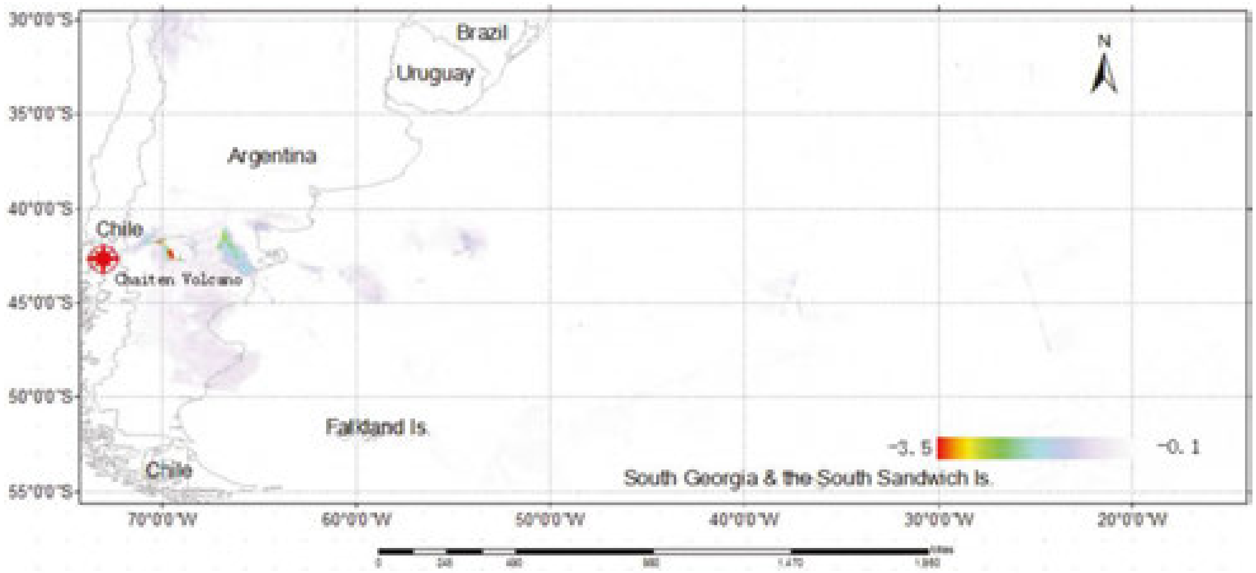

Figure 11. May 9, 18:10 UT: Chile (MODIS).

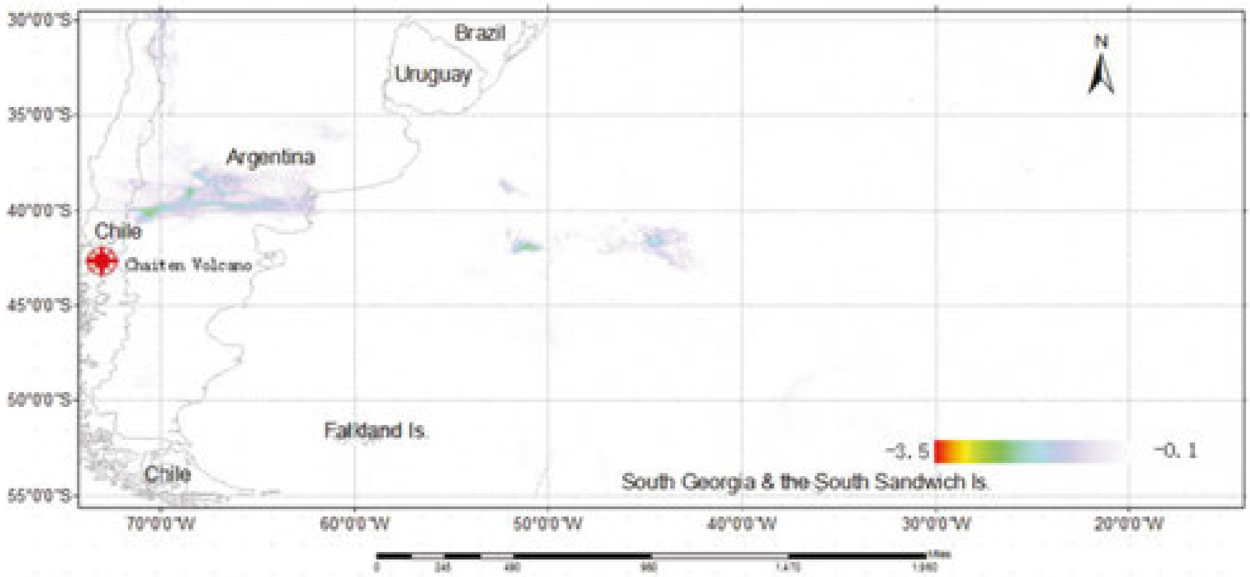

Figure 12. May 10, 14:40 UT: Chile (MODIS).

4. Results and discussion

4.1. Eruption cloud tracking

Applying Eqs (3) and (4), the eruption cloud tracking BTD images can be calculated from MODIS images data shown as in **Figures 13–20**.

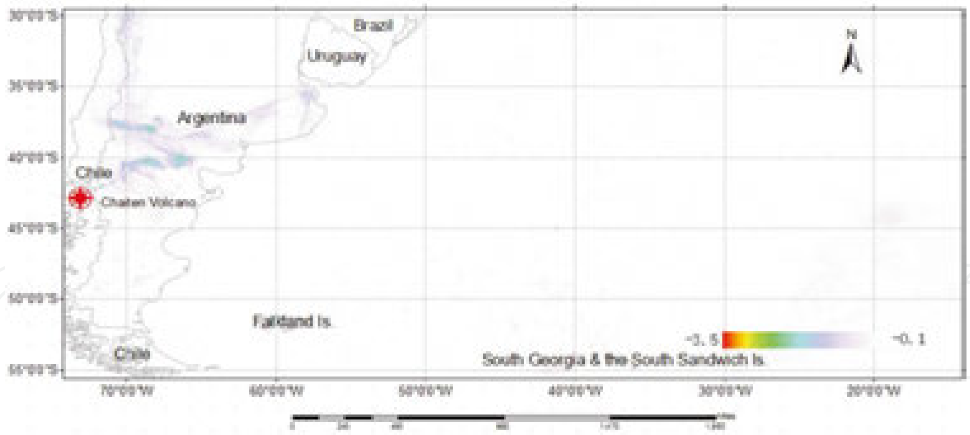

Figure 13. Chaitén eruption cloud on 3 May 2008.

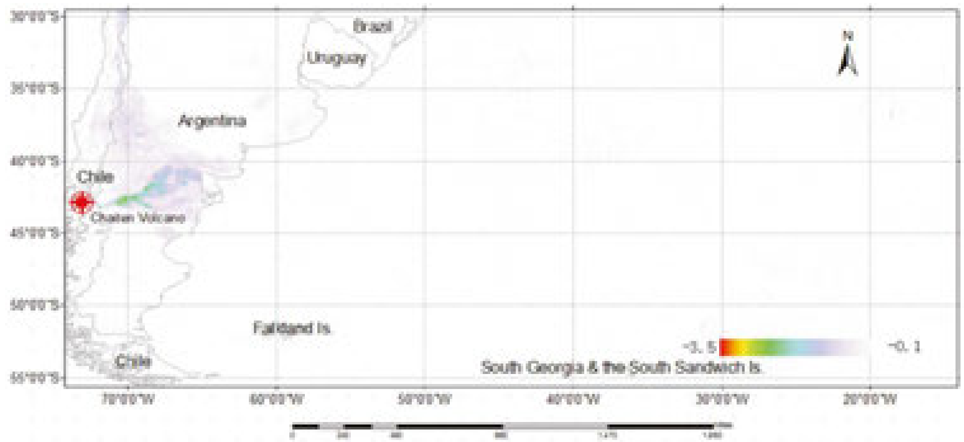

Figure 14. Chaitén eruption cloud on 4 May 2008.

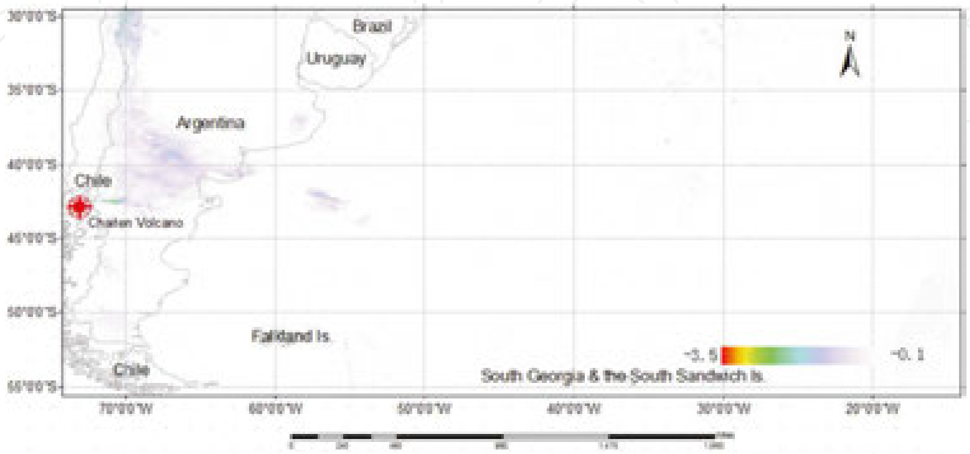

Figure 15. Chaitén eruption cloud on 5 May 2008.

http://dx.doi.org/10.5772/00000

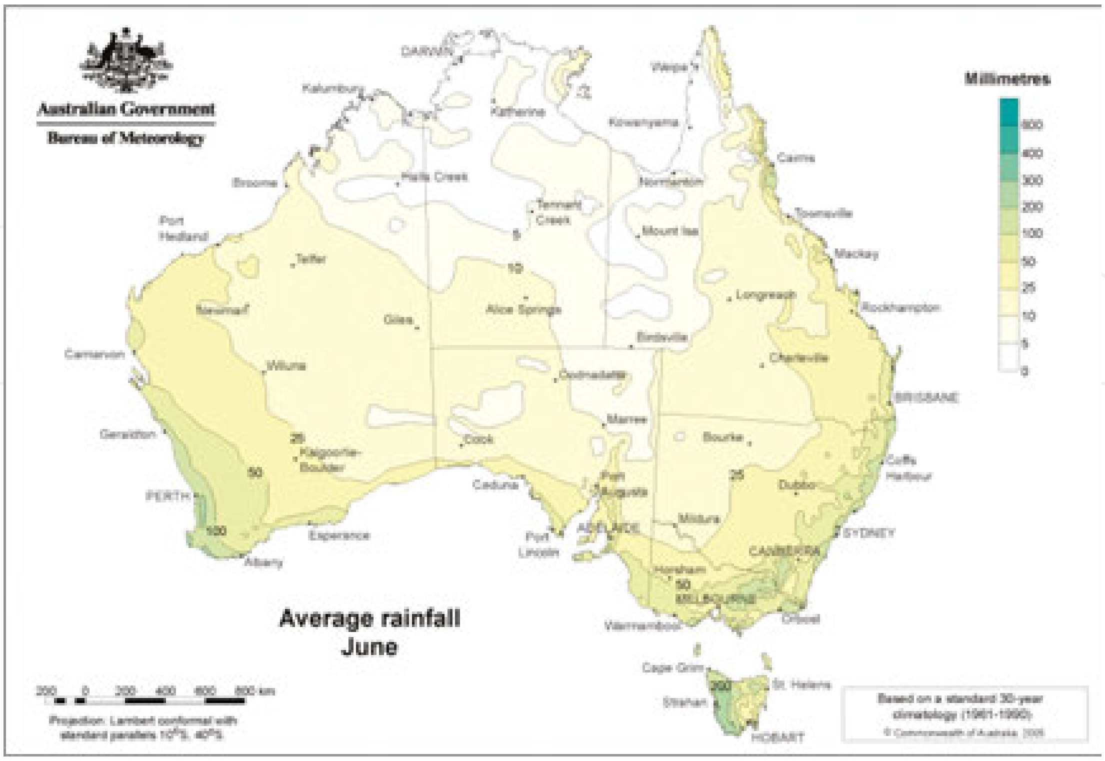

Figure 16. Chaitén eruption cloud on 6 May 2008.

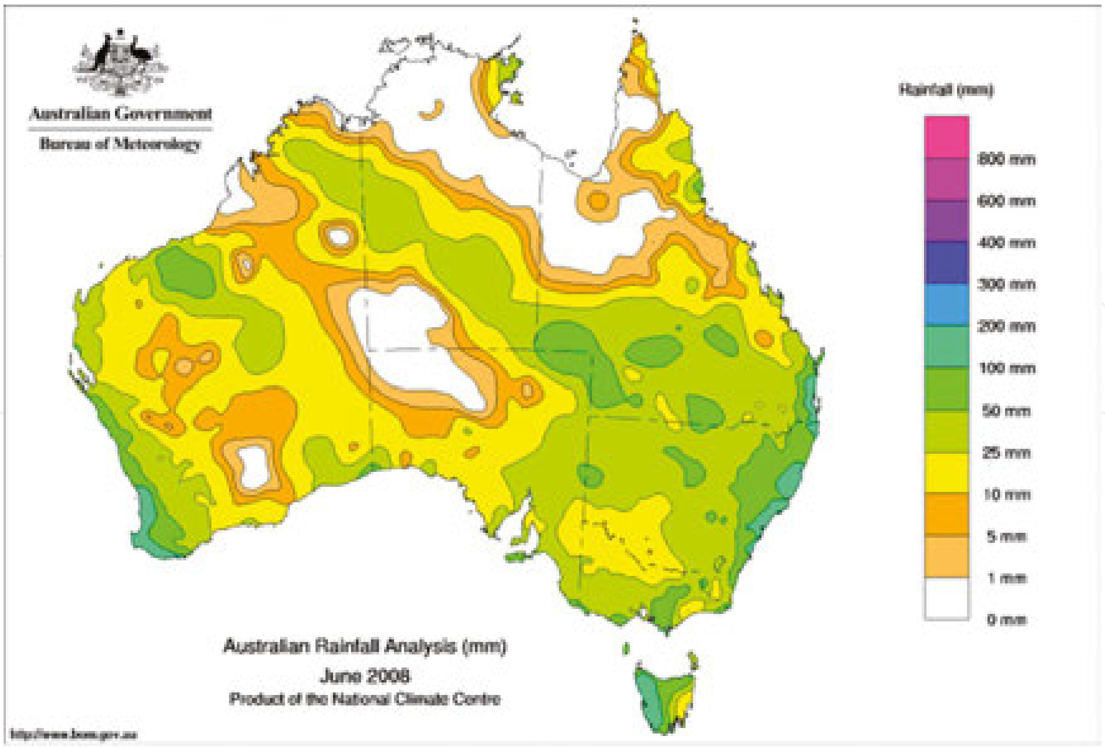

Figure 17. Chaitén eruption cloud on 7 May 2008.

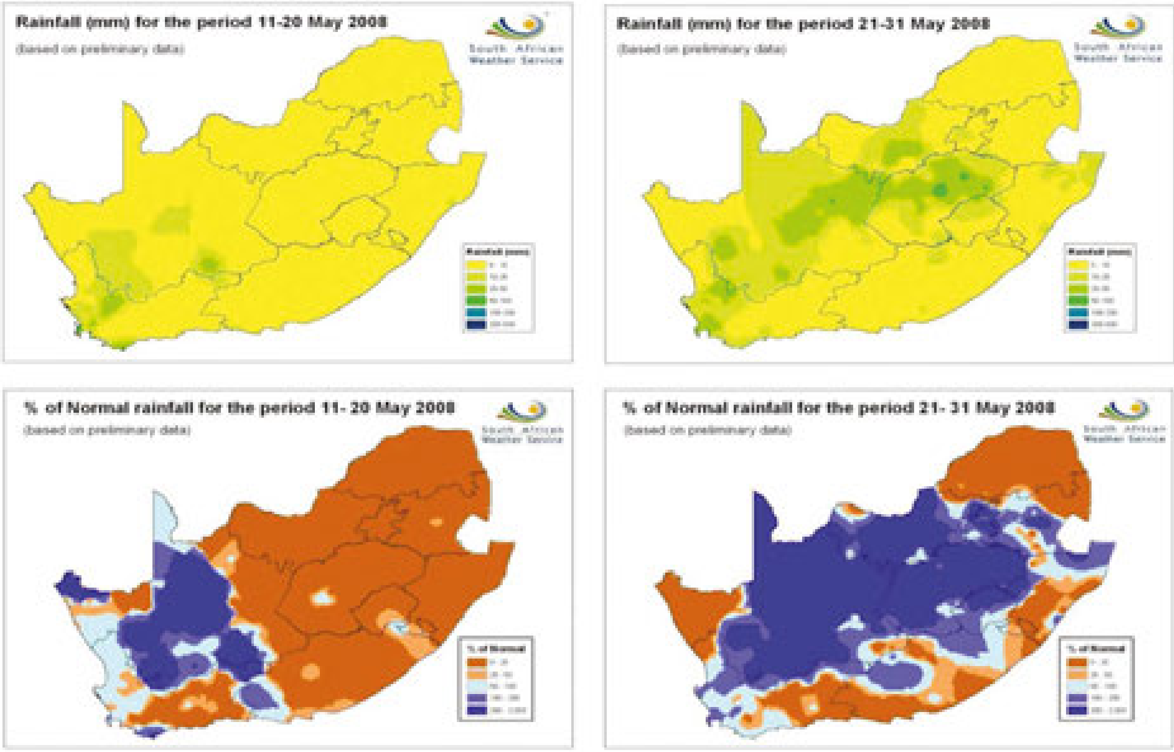

Figure 18. Chaitén eruption on 8 May 2008.

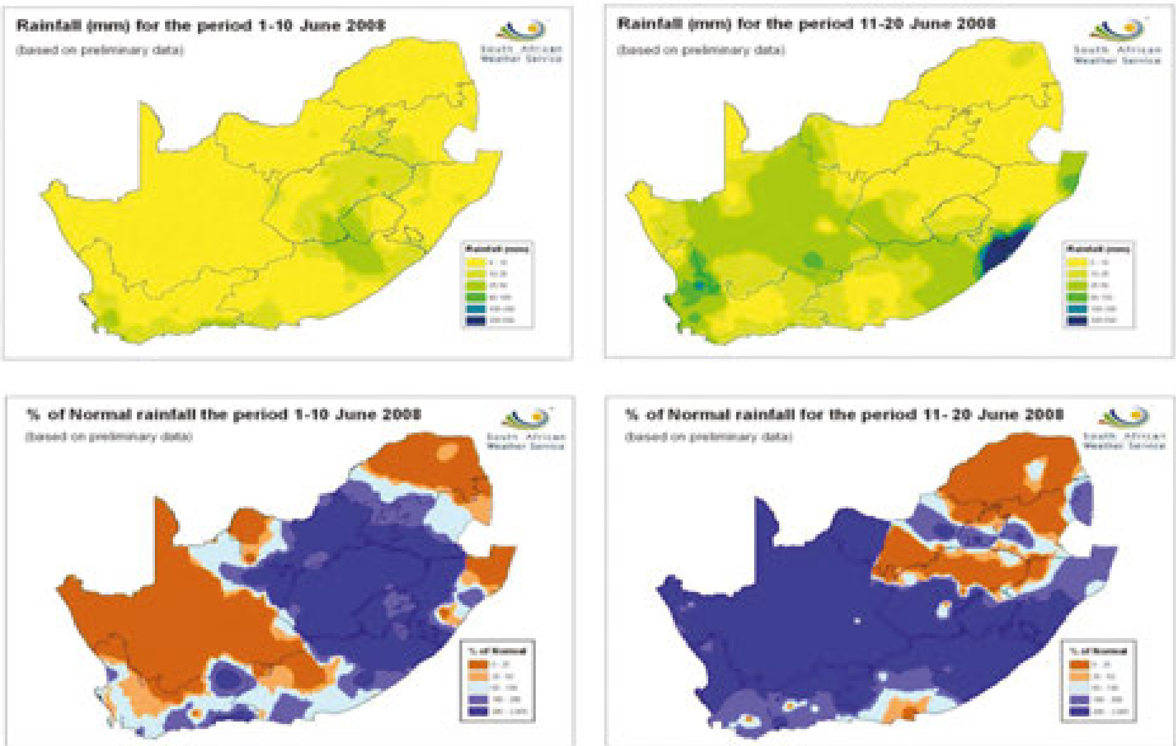

Figure 19. Chaitén eruption cloud on 9 May 2008.

http://dx.doi.org/10.5772/00000

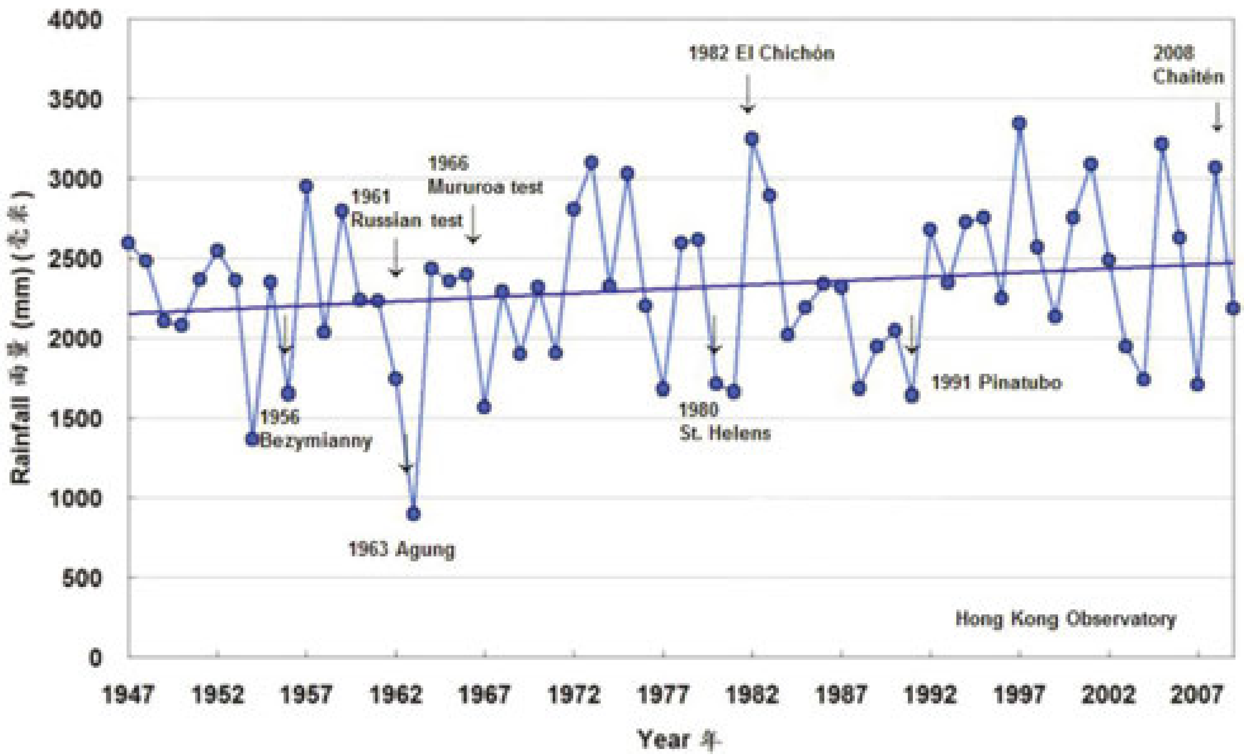

Figure 20. Chaitén eruption cloud on 10 May 2008.

Based on the results of monitoring the volcanic ashes using MODIS in this study and the referred reports, the following inferences can be drawn as below:

(1) On 3 May (**Figure 13**)—The eruption cloud formed a continuous, linear, and sharp-edged plume. The cloud-drifted southeastward reaching the Atlantic coast of Argentina

(2) On 4 May (**Figure 14**)—The volcanic ash fallout direction is toward the southeast which is similar to 3 May. The Chilean town of Futaleufu, located at about 75 km from the volcano, received copious fallout where ash deposition of10–30 cm in thickness is reported in [23] (3) On 5 May (**Figure 15**)—A continuous linear plume with an easterly orientation passed over the Atlantic Ocean. Large quantities of fine ash were reported at Trelew, Rawson and Madryn in [23] in Argentina and several Argentinian regional airports were shut down due to the lack of visibility.

(4) On 6 May (**Figure 16**)—It is reported that the eruption entered a more intense but short-lived phase with column height up to 30 km estimated. This eruption produced a cloud that drifted northeastwards across the Andes into Argentina.

(5) On 7 May (**Figure 17**)—The eruption cloud continued to drift in a northeast direction. Light fallout was reported at Bahia Blanca and Mar del Plata in Argentina in [23], located at more than 1000 km away from the volcano.

(6) On 8 May (**Figure 18**)—The eruption cloud moved in a northeasterly and northerly direction.

(7) On 9 May (**Figure 19**)—There was an increase in eruption activity on 9 May compared to 8 May. The volcanic ash drifted northeastwards reaching the Atlantic coast of Argentina.

(8) On 10 May (**Figure 20**)—A light eruption occurred on 10 May and the volcanic ash drifted eastwards.

4.2. Precipitation impact further downstream

Two examples of downstream precipitation impact over the continent of Australia are shown in **Figures 2** and **3**. It can be clear that the rainfall in June 2008 was much more over that of the Australian continent in the average of 1961–1990 normal. The link with the spread of the Chaitén eruption cloud is supported by the detection of stratospheric aerosol drifting over southeastern Australia by Cloud-Aerosol Lidar with Orthogonal Polarization (CALIOP) in [2]. Similarly torrential June rainfall occurred in South Africa (**Figure 5**) and over Hong Kong (**Figure 6**) in southern China in [24]. From **Figures 4** and **5**, it is obviously that late May, early and middle June 2008 in South Africa, the rainfall had a significant increase compared with that early May. It is reported that heavy rainfall on June 19 across parts of South Africa prompted severe flooding and mudslides. According to reports, Scottburgh, KwaZulu-Natal received a total of 128 mm of rain within 24-h (NOAA). June 2008 in Hong Kong with 1364.1 mm rainfall was the wettest month since record began in 1884. This included a rainstorm with a return period of 1100 years which led to over 2400 landslides on Lantau Island in [25]. The spread of stratospheric aerosols across the Intertropical Convergence Zone was likely to have been assisted by the timing of the early May eruption date which was during the southern hemisphere autumn when solar radiation intensity was decreasing in the southern hemisphere and increasing in the northern hemisphere.

5. Conclusions and future work

We have tracked the transport and deposition of volcanic ash during the first 8 days of May 2008 Chaiten volcano activity in Chile from 3 May to 10 May using MODIS images. The purpose was to learn the dispersion pattern of the eruption cloud and to analyze the possible impacts on rainfall. The volcanic ash detection procedure used in this study is based on the BTD algorithm using the thermal infrared channels centered on 11 and 12 μm of a multispectral satellite sensor. The results of BTD volcanic ash retrieval algorithm have been found to show good agreement with RGB images recorded by NASA-MODIS Terra and Aqua sensors. The eruption cloud was found to drift northeastwards, southeastwards and eastwards following the eruptions, reaching the Atlantic coast of Argentina and beyond over a 8-day period. The timing of heavy rainfall during May/June in South Africa, during June 2008 in central Australia and during June in Hong Kong (the wettest since record began in 1884) was thought to have been connected to the dispersion of particulates further downstream. However, the effective radius of volcanic ash particles and optical depths of clouds detection were not included in this research, but will be considered in our future work.

http://dx.doi.org/10.5772/00000

Acknowledgements

This research is supported by an Open Research Program at State Key Laboratory of Geological Processes and Mineral Resources (GPMR), China University of Geosciences in 2015. MODIS images data from NASA, rainfall images of Australian and South Africa from Australian Bureau of Meteorology and from the website of South Africa Weather Service, and the Hong Kong's annual rainfall data from Hong Kong Observatory (HKO) were acknowledged. The reviewer and editor's critical comments are helpful for improving the manuscript.

Author details

Yuanzhi Zhang[1,2*], Jin Yeu Tsou[2], Zhaojun Huang[2], Jinrong Hu[2] and Wyss W.-S. Yim[3]

*Address all correspondence to: yuanzhizhang@hotmail.com

1 Key Lab of Lunar and Deep-Space Exploration, Chinese Academy of Sciences, Beijing, China

2 Center for Housing Innovations, the Chinese University of Hong Kong, Shatin, Hong Kong

3 Department of Earth Sciences, the University of Hong Kong, Pok Fu Lam, Hong Kong

References

[1] Ellrod, G. P. and Connell, B. H., 2003. Improved detection of airborne volcanic ash using multispectral infrared satellite data, J. Geophys. Res., Vol. 108(D12), 4356.

[2] Carn, S. A., Pallister, J. S., Lara, L., Ewert, J. W., Watt, S., Prata, A. J., Thomas, R. J. and Villarosa, G. 2009. The unexpected awakening of Chaitén volcano, Chile, EOS Trans., Vol. 90(24), 205–206.

[3] Watt, F. L. and Pyle, D. M., 2009. Fallout and distribution of volcanic ash over Argentina following the May 2008 explosive eruption of Chaitén, Chile, J. Geophys. Res., Vol. 114, B04207, doi:10.1029/2008JB006219.

[4] Lara, L. E., 2009. The 2008 eruption of the Chaitén volcano, Chile: a preliminary report, Andean Geol., Vol. 36(1), 125–129.

[5] Scasso, R., Corbell, H., and Tiberi, T., 1994. Sedimentological analysis of the tephra from the 12–15 August 1991 eruption of Hudson volcano, Bull. Volcanol., Vol. 56, 121–133.

[6] Naranjo, J. and Stern, C., 2004. Holocene tephrochronology of the southern most Part (42°30′-45°S) of the Andean Southern Volcanic Zone, Revista Geolgica de Chile, Vol. 31, 225–240.

[7] Guffanti, M., Benitez, C., Andrioli, M., Romero, R. and Casadevall, T. J., 2008. Widespread effects on aviation of the 2008 eruption of Chaitén volcano, Chile, EOS Trans. AGU, Vol. 89(53), Fall Meet. Suppl., Abstract, V42C-03.

[8] NOAA: http://www.ncdc.noaa.gov/sotc/hazards/2008/6

[9] Prata, A. J., 1989a. Observations of volcanic ash clouds in 10–12 μm window using AVHRR/2 data, Int. J. Remote Sens., Vol. 10, 751–761.

[10] Prata, A. J., 1989b. Infrared radiative transfer calculations for volcanic ash clouds, Geophys. Res. Lett., Vol. 16(11), 1293–1296.

[11] Wen, S. and Rose, W. I., 1994. Retrieval of sizes and total masses of particles in volcanic clouds using AVHRR bands 4 and 5, J. Geophys. Res., Vol. 99(D3), 5421–5431.

[12] Hillger, D. W. and Clark, J. D., 2002. Principal component image analysis of MODIS for volcanic ash. Part I: most important bands and implications for future GOES imagers, J. Appl. Meteorol., 41, 985–1001.

[13] Watson, I. M., Realmuto, V. J., Rose, W. I., Prata, A. J., Bluth,G. J. S., Gu, Y., Bader, C. E., and Yu, T., 2004. Thermal infrared remote sensing of volcanic emissions using the moderate resolution imaging spectroradiometer, J. Volcanol. Geoth. Res., 135, 75–89.

[14] Tupper, A., Carn, S., Davey, J., Kamada, Y., Potts, R., and Prata, F., 2004. An evaluation of volcanic cloud detection techniques during recent significant eruption in the western Ring of Fire, Remote Sens. Environ., 91, 27–46.

[15] Corradini, S., Spinetti, C., Carboni, E., Tirelli, C., Buongiorno, M. F., Pugnaghi, S., and Gangale, G., 2008a. Mt. Etna tropospheric ash retrievaland sensitivity analysis using Moderate Resolution Imaging Spectroradiometer measurements, J. Atmos. Remote. Sens., 2, 023550, doi:10.1117/1.3046674.

[16] Corradini, S., Merucci, L., Prata, A. J., and Piscini, A., 2010. Volcanic ash and SO_2 in the 2008 Kasatochi eruption: retrievals comparison from different IR satellite sensors, J. Geophys. Res., 115, D00L21, doi:10.1029/2009JD013634.

[17] Corradini, S., Merucci, L., and Arnau, F., 2011. Volcanic ash cloud properties: comparison between MODIS satellite retrievals and FALL3D transport model, IEEE Geosci. Remote Sens. Lett., 8, 248–252.

[18] Yu T, Rose W. I., Prata A. J. 2002. Atmospheric correction for satellite-based volcanic ash mapping and retrievals using split window IR data from GEOS and AVHRR, J. Geophys. Res. 107 (D16):4311.doi:10.1029/2001JD000706.

[19] Prata, A. J. and Kerkmann, J 2007. Simultaneous retrieval of volcanic ash and SO_2 using MSG-SEVIRI measurements. Geophys. Res. Lett., 34:L05813.doi: 10.1029/2006GL028691.

[20] Pujol, G. C., Rabolli, M., Kalemkarian, M., 2008. Volcanic ash detection, monitoring and environment impact, Servicio Metorologico. Macional. (SMN), 7–17.

[21] Spinetti, C. and Corradini, S., 2007. Volcanic ash retrieval at Mt. Etna using AVHRR and MODIS data, Proc. of SPIE, Vol. 6749, 1–3.

[22] Jiang, L. P. and Qin, Z. H., 2006. Program splits window algorithm to retrieve land surface temperature for MODIS data using IDL, Geomat. Spat.l Inf. Technol., Vol. 29, No.3 Jun., 115–116.

[23] Folch, A., Jirba, O. and Viramonte, J., 2008. Volcanic ash forecast-application to the May 2008 Chaiten eruption, Nat. Hazards Earth Syst. Sci., 8, 927–940.

[24] Yim, W. 2010. Chilean volcano produces trail of destruction. Imperial Engineer, 12(Spring), 10–11.

[25] Kwan, J. S. H., Hui, T. H. H. and Ho, K. K. S., 2011. Modelling the motion of mobile debris flows in Hong Kong. Proc. of Second World Landslide Forum, 3–7 October 2011, Rome, 6 p.